JOURNAL OF SOLID STATE CHEMISTRY **130,** 48–53 (1997)
ARTICLE NO. SC977273

Mixed Valent Molybdenotungsten Monophosphate $Rb_2Mo_2WO_5(PO_4)_3$: An Interconnected Tunnel Structure

A. Leclaire, M. M. Borel, J. Chardon, and B. Raveau

Laboratoire CRISMAT, URA 1318 associée au CNRS, ISMRA et Université de Caen, Bd du Maréchal Juin, 14050 Caen Cedex, France

Received July 18, 1996; in revised form January 3, 1997; accepted January 8, 1997

A new mixed valent molybdenotungsten monophosphate $Rb_2Mo_2WO_5(PO_4)_3$ has been synthesized. It crystallizes in the $P2_1/n$ space group with $a=10.756(2)$ Å, $b=9.493(1)$ Å, $c=15.478(3)$ Å, $\beta=108.99(2)^\circ$. The structure of this phase consists of corner-sharing single MO_6 octahedra, M_2O_{11} bioctahedral units, and monophosphate PO_4 groups forming large interconnected tunnels running along b and a where the rubidium cations are located. The complex host lattice $[Mo_2WP_3O_{17}]_\infty$ can be described by the assemblage of enantiomorphic $[M_3P_3O_{20}]_\infty$ chains running along a. A preferential occupation of two out of three octahedral sites by molybdenum is observed and a distribution of the hexavalent and pentavalent species in these different sites is proposed. The rather large Rb–O distances observed for the three kinds of rubidium sites suggest possible mobility of the Rb^+ cations in agreement with their high thermal factors. © 1997 Academic Press

INTRODUCTION

The investigations of molybdenum phosphates (see for review Refs. 1 and 2) and of tungsten phosphates (see for review Ref. 3) performed in the past 20 years have shown the extraordinary richness of the crystal chemistry of these compounds that are susceptible to exhibit interesting electron transport properties (see for instance Ref. 4). Very recently, a new field of research has been opened with the discovery of mixed valent molybdenotungsten phosphates (5–10) with original structure, different from those of the pure molybdenum or pure tungsten phosphates. Two sodium monophosphates $Na_x(Mo,W)O_3(PO_4)_2$ (5) and $Na_{1+x}(Mo,W)O_5PO_4$ (6), two lithium monophosphates $Li(Mo,W)_2O_3(PO_4)_2$ (7) and $Li_x(Mo,W)_2O_3(PO_4)_2$ (8), and two potassium monophosphates $K_{6.6}Mo_{2.36}W_{3.64}O_{15}(PO_4)_4$ (9) and $K_6Mo_3W_9PO_{40}\cdot 13H_2O$ (10) have indeed been isolated in the past 2 years.

No molybdenotungsten phosphate containing large univalent cations such as rubidium, thallium, or cesium has been synthesized to date. Such compounds, if they exist, should exhibit an opened framework as shown from the studies of the potassium phases (9, 10). To understand the crystal chemistry of these new molybdenotungsten phosphates, we have investigated the system Rb–Mo–W–P–O. In the present paper, we describe the structure of a new mixed valent molybdenotungsten monophosphate $Rb_2Mo_2WO_5(PO_4)_3$ that possesses interconnected tunnels.

CRYSTAL GROWTH

Single crystals of the title compound were grown from a mixture of nominal composition $Rb_3Mo_{3.5}W_{1.5}P_5O_{27}$. The growth was carried out in two steps: first $H(NH_4)_2PO_4$, $RbNO_3$, WO_3, and MoO_3 were mixed in an agate mortar in adequate ratios according to the composition $Rb_3Mo_{2.83}W_{1.5}P_5O_{27}$ and heated at 700 K in a platinum crucible to decompose the ammonium phosphate and nitrate. In a second step the resulting mixture was then added to the required amount of molybdenum (0.17 mole), sealed in an evacuated silica ampoule, heated for a day at 823 K, and cooled at 2 K per hour to 773 K; the sample was finally quenched to room temperature.

From the resulting product some orange crystals were extracted. The latter were studied by X-ray diffraction and their microprobe analysis confirmed the composition $Rb_2Mo_2WP_3O_{17}$ deduced from the structure determination.

Attempts to prepare the phase $Rb_2Mo_2WP_3O_{17}$ starting from the nominal composition led to the expected powder X-ray pattern but always with some extra lines due to unidentified impurities.

STRUCTURE DETERMINATION

An orange crystal with dimensions $0.104\times0.052\times0.060$ mm was selected for structure determination. The cell parameters reported in Table 1 were determined and refined by diffractometric technique at 294 K with a least square refinement based on 25 reflections with $18^\circ \le \theta \le 22^\circ$. The

0022-4596/97 $25.00

systematic absences $h + l = 2n + 1$ for $h0l$ and $k = 2n + 1$ for $0k0$ are consistent with the space group $P2_1/n$. The data were collected with an Enraf-Nonius CAD4 diffractometer with the parameters reported in Table 1. The reflections were corrected for Lorentz and polarization effects and for absorption.

The structure was solved with the heavy atom method. The W and Mo atoms are distributed over three sites $M(1)$, $M(2)$, and $M(3)$. The refinement of the occupancy factors of the metallic sites shows that the $M(1)$ sites are preferentially occupied by tungsten 0.572W/0.428Mo whereas the $M(2)$ and $M(3)$ sites are essentially occupied by molybdenum, i.e., 0.328W/0.672Mo and 0.117W/0.883Mo, respectively.

The difference synthesis and the occupancy refinement show that three sites are available for the rubidium: Rb(1) is fully occupied whereas Rb(2) is spread over two close-set sites Rb(21) and Rb(22), the occupations of which are 0.25 and 0.75, respectively. Attempts to refine anisotropic thermal factors for Rb(21) and Rb(22) lead to undefined non-convergent factors which were strongly correlated. So in the further refinements, isotropic thermal factors were used for Rb(21) and Rb(22).

The refinement of the atomic coordinates of the isotropic thermal factor of oxygen atoms and anisotropic thermal factors of all the other atoms leads to $R = 0.046$ and $R_w = 0.048$, for the atomic coordinates listed in Table 2.

TABLE 1
Summary of Crystal Data, Intensity Measurements, and Structure Refinement Parameters for $Rb_2Mo_2WO_5(PO_4)_3$

1. Crystal data	
Space group	$P2_1/n$
Cell dimensions	$a = 10.756(2)$ Å $\alpha = 90°$
	$b = 9.493(1)$ Å $\beta = 108.99(2)°$
	$c = 15.478(3)$ Å $\gamma = 90°$
Volume (Å)^3	1494.4(4) Å^3
Z	4
ρ_{calc} (gm^3)	4.05
2. Intensity measurements	
λ(Mo$K\alpha$)	0.71073
Scan mode	ω–θ
Scan width (°)	$1.4 + 0.35 \tan\theta$
Slit aperture (mm)	$1.2 + \tan\theta$
max θ(°)	45
Standard reflections	3 measured every 3600 s
Reflections with $I > 3\sigma$	2499
μ(mm^{-1})	16.25
3. Structure solution and refinement	
Parameters refined	145
Agreement factors	$R = 0.046$, $R_w = 0.048$
Weighting scheme	$w = 1/\sigma^2$
Δ/σ max	< 0.01

TABLE 2
Positional Parameters and Their Estimated Deviations in $Rb_2Mo_2WO_5(PO_4)_3$ and Atomic Anisotropic Displacement Parameters

Atom	x	y	z	B (Å^2)	Occupancy
$M(1)^a$	0.31228(8)	0.1226(1)	0.06091(5)	0.54(3)[d]	1.0
$M(2)^b$	0.4765(1)	0.2544(1)	0.40162(6)	0.77(3)[d]	1.0
$M(3)^c$	0.8019(1)	0.1197(1)	0.25667(7)	0.62(3)[d]	1.0
Rb(1)	0.1032(2)	0.3691(2)	0.2107(1)	2.19(6)[d]	1.0
Rb(21)	0.208(2)	0.097(2)	0.4927(8)	3.9(4)	0.25(2)
Rb(22)	0.1635(7)	0.1363(7)	0.4937(2)	3.4(2)	0.75(2)
P(1)	0.0779(4)	0.5976(4)	0.6219(3)	0.64(8)[d]	1.0
P(2)	0.4021(4)	0.4034(5)	0.5699(3)	0.72(8)[d]	1.0
P(3)	0.5381(4)	0.3248(5)	0.2007(3)	1.0(8)[d]	1.0
O(1)	0.250(1)	0.116(1)	0.1496(7)	1.1(8)	1.0
O(2)	0.191(1)	0.217(1)	− 0.0206(7)	1.1(8)	1.0
O(3)	0.232(1)	− 0.056(1)	0.0005(7)	0.7(8)	1.0
O(4)	0.421(1)	0.291(1)	0.1144(7)	1.0(8)	1.0
O(5)	0.462(1)	− 0.006(1)	0.1291(7)	0.7(8)	1.0
O(6)	0.437(1)	0.137(1)	− 0.0242(7)	1.0(8)	1.0
O(7)	0.312(1)	0.251(1)	0.3543(7)	1.4(8)	1.0
O(8)	0.515(1)	0.081(1)	0.4211(8)	1.3(8)	1.0
O(9)	0.464(1)	0.289(1)	0.5270(7)	0.8(8)	1.0
O(10)	0.515(1)	0.261(1)	0.2840(7)	1.0(8)	1.0
O(11)	0.509(1)	0.471(1)	0.4025(8)	1.2(8)	1.0
O(12)	0.743(1)	0.078(1)	0.3418(8)	1.5(8)	1.0
O(13)	0.711(1)	− 0.026(1)	0.1659(7)	0.8(8)	1.0
O(14)	0.958(1)	− 0.015(1)	0.2974(7)	1.2(8)	1.0
O(15)	0.665(1)	0.262(1)	0.1921(7)	0.9(8)	1.0
O(16)	0.929(1)	0.268(1)	0.3228(7)	1.1(8)	1.0
O(17)	0.881(1)	0.172(1)	0.1506(7)	0.9(8)	1.0

	U_{11}	U_{22}	U_{33}	U_{12}	U_{13}	U_{23}
W(1)	0.0089(4)	0.0074(4)	0.0044(4)	0.0006(4)	0.0025(3)	− 0.0007(4)
Mo(1)	0.0089(4)	0.0074(4)	0.0044(4)	0.0006(4)	0.0025(3)	− 0.0007(4)
W(2)	0.0140(5)	0.0093(5)	0.0049(4)	− 0.0021(5)	0.0056(3)	− 0.0016(4)
Mo(2)	0.0140(5)	0.0093(5)	0.0049(4)	− 0.0021(5)	0.0056(3)	− 0.0016(4)
W(3)	0.0113(6)	0.0079(6)	0.0048(5)	− 0.0001(6)	0.0037(4)	− 0.0017(5)
Mo(3)	0.0113(6)	0.0079(6)	0.0048(5)	− 0.0001(6)	0.0037(4)	− 0.0017(5)
Rb(1)	0.034(1)	0.029(1)	0.0170(8)	− 0.003(1)	0.0052(7)	0.0008(9)
P(1)	0.013(2)	0.005(2)	0.005(2)	− 0.000(2)	0.003(2)	− 0.001(1)
P(2)	0.016(2)	0.010(2)	0.004(2)	0.001(2)	0.006(2)	0.000(1)
P(3)	0.016(2)	0.012(2)	0.008(2)	− 0.001(2)	0.005(2)	0.001(2)

[a] $M(1) = Mo_{0.428(9)}W_{0.572(9)}$.
[b] $M(2) = Mo_{0.672(8)}W_{0.328(8)}$.
[c] $M(3) = Mo_{0.883(7)}W_{0.117(7)}$.
[d] Atom anisotropically refined. Anisotropically refined atoms are given in the form of the isotropic equivalent displacement parameter defined as

$$B = \frac{4}{3}\sum_i\sum_j \mathbf{a}_i\mathbf{a}_j\beta_{ij}.$$

DESCRIPTION OF THE STRUCTURE

The projection of the $[Mo_2WP_3O_{17}]_\infty$ framework along **b** shows its complexity (Fig. 1). It consists of bioctahedral

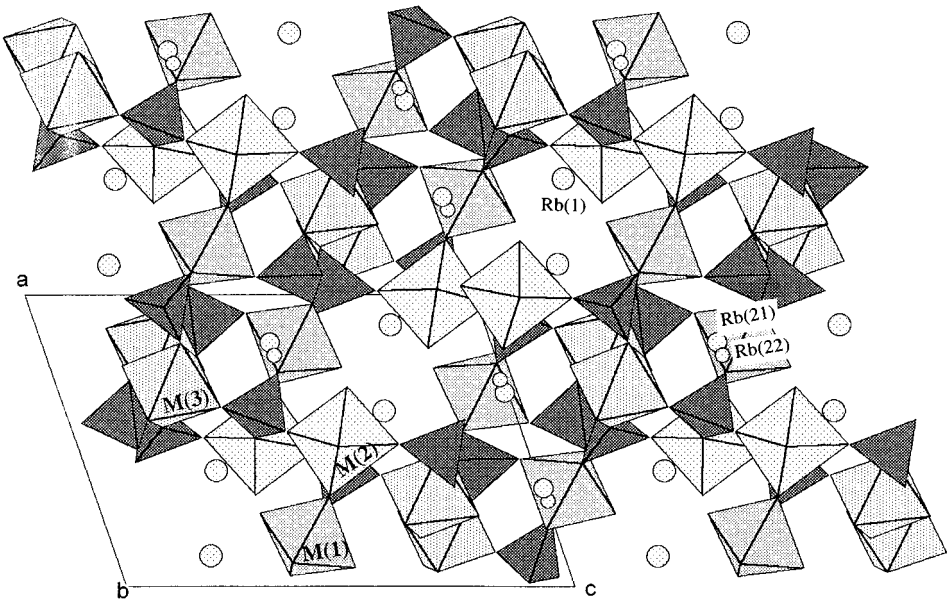

FIG. 1. The projection of the $[Mo_2WP_3O_{17}]_\infty$ framework along **b**.

units M_2O_{11} involving two kinds of octahedra $M(1)$ and $M(2)$ and single MO_6 octahedra labeled $M(3)$, sharing their apices with PO_4 monophosphate groups. These polyhedra delimit large cross-shaped tunnels running along **b**, where rubidium cations (labeled Rb(1)) are located.

The whole structure can in fact be described by the stacking along **b** of layers built from identical disconnected waving chains $[M_3P_3O_{20}]_\infty$ running along **a** (Fig. 2a). In these chains, the bioctahedral units "$M(1)M(2)$" and the single $M(3)$ octahedra are linked through the PO_4 tetrahedra in a complex way. Each P(1) tetrahedron shares two apices with $M(1)$ octahedra of two different bioctahedral units and one apex with one $M(3)$ isolated octahedron. Each P(2) tetrahedron shares two apices with the same bioctahedral unit, i.e., with $M(1)$ and $M(2)$, respectively, one apex with one $M(2)$ octahedron of another bioctahedral unit, and the fourth apex with one $M(3)$ isolated octahedron. The P(3) tetrahedron is linked to one isolated $M(3)$ octahedron and to one $M(2)$ octahedron.

Two successive (010) layers of polyhedra exhibit enantiomorphic $[M_3P_3O_{20}]_\infty$ chains as shown in Fig. 2b. Moreover the chains of two adjacent layers are shifted by

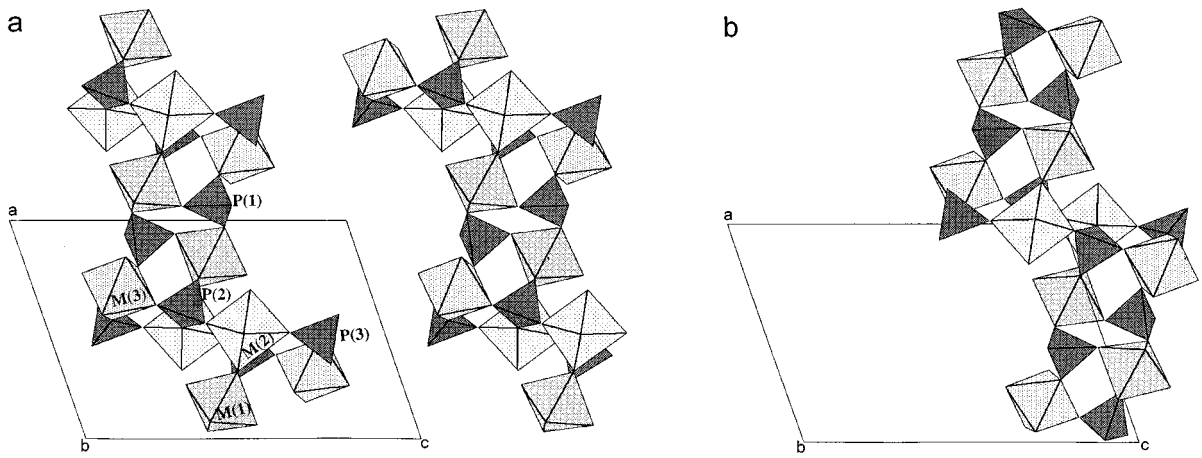

FIG. 2. (a) The (010) layer of polyhedra built from waving chains $[M_3P_3O_{20}]_\infty$ running along **a**. (b) The enantiomorphic $[M_3P_3O_{20}]_\infty$ chain.

TABLE 3
Distances (Å) and Angles (°) in the Polyhedra in $Rb_2Mo_2WO_5(PO_4)_3$

M(1)	O(1)	O(2)	O(3)	O(4)	O(5)	O(6)
O(1)	**1.71(1)**	2.68(2)	2.78(2)	2.65(2)	2.66(2)	3.85(2)
O(2)	101.9(5)	**1.73(1)**	2.63(2)	2.75(2)	3.73(2)	2.76(2)
O(3)	97.0(5)	89.3(4)	**1.99(1)**	3.97(2)	2.67(2)	2.99(2)
O(4)	91.3(5)	95.1(5)	169.6(5)	**1.90(1)**	2.85(2)	2.65(2)
O(5)	90.7(5)	166.1(5)	83.4(4)	90.3(4)	**2.02(1)**	2.67(2)
O(6)	165.7(4)	89.5(5)	91.7(5)	79.0(5)	79.0(3)	**2.17(1)**
M(2)	O(7)	O(8)	O(9)	O(10)	O(11)	$O(2)^{i}$
O(7)	**1.68(1)**	2.64(2)	2.67(2)	2.75(2)	2.89(2)	3.92(2)
O(8)	102.7(6)	**1.70(1)**	2.73(2)	2.72(2)	3.71(2)	2.64(2)
O(9)	91.8(5)	94.2(5)	**2.01(1)**	3.98(2)	2.75(2)	2.77(2)
O(10)	96.2(5)	94.6(6)	166.5(4)	**2.00(1)**	2.72(2)	3.01(2)
O(11)	100.0(6)	157.3(5)	84.2(5)	83.7(5)	**2.08(1)**	2.63(2)
$O(2)^{i}$	171.4(5)	82.7(5)	80.9(4)	90.0(4)	74.7(4)	**2.25(1)**
M(3)	O(12)	O(13)	O(14)	O(15)	O(16)	O(17)
O(12)	**1.68(1)**	2.81(2)	2.76(2)	2.81(2)	2.78(2)	3.82(2)
O(13)	99.5(5)	**1.99(1)**	2.78(2)	2.83(2)	3.93(2)	2.69(2)
O(14)	95.3(5)	87.2(4)	**2.04(1)**	4.02(2)	2.75(2)	2.79(2)
O(15)	98.5(5)	90.2(4)	166.2(5)	**2.01(1)**	2.90(2)	2.74(2)
O(16)	97.6(5)	162.0(5)	85.8(4)	92.7(4)	**1.99(1)**	2.71(2)
O(17)	178.7(5)	81.2(4)	83.6(5)	82.6(4)	81.5(4)	**2.14(2)**
P(1)	$O(6)^{ii}$	$O(16)^{iii}$	$O(5)^{iv}$	$O(13)^{iv}$		
$O(6)^{ii}$	**1.52(1)**	2.51(2)	2.55(2)	2.48(2)		
$O(16)^{iii}$	109.9(6)	**1.55(1)**	2.44(2)	2.51(2)		
$O(5)^{iv}$	112.6(6)	103.9(6)	**1.55(1)**	2.55(2)		
$O(13)^{iv}$	109.4(6)	109.0(6)	111.8(6)	**1.53(1)**		
P(2)	O (9)	$O(3)^{ii}$	$O(11)^{iii}$	$O(17)^{iv}$		
O(9)	**1.54(1)**	2.49(2)	2.51(2)	2.39(2)		
$O(3)^{ii}$	107.9(6)	**1.54(1)**	2.52(2)	2.51(2)		
$O(11)^{iii}$	111.1(7)	111.3(6)	**1.51(1)**	2.53(2)		
$O(17)^{iv}$	102.7(7)	110.1(7)	113.1(6)	**1.52(1)**		
P(3)	O(4)	O(10)	O(15)	$O(14)^{v}$		
O(14)	**1.55(1)**	2.50(2)	2.52(2)	2.41(2)		
O(10)	109.8(7)	**1.51(1)**	2.47(2)	2.54(2)		
O(15)	110.2(7)	108.4(6)	**1.53(1)**	2.53(2)		
$O(14)^{v}$	103.6(6)	113.1(7)	111.8(7)	**1.52(1)**		

Rb(1)–O(1): 3.18(2)
Rb(1)–$O(1)^{ii}$: 3.23(2)
Rb(1)–$O(5)^{ii}$: 3.03(2)
Rb(1)–O(7): 2.83(2)
Rb(1)–$O(8)^{ii}$: 2.85(2)
Rb(1)–$O(9)^{vi}$: 3.13(2)
Rb(1)–$O(16)^{vii}$: 3.09(2)
Rb(1)–$O(17)^{vii}$: 2.93(2)

Rb(21)–$O(3)^{ii}$: 3.35(2)
Rb(21)–$O(4)^{ii}$: 3.41(2)
Rb(21)–O(7): 3.09(2)
Rb(21)–$O(8)^{viii}$: 3.31(2)
Rb(21)–O(9): 3.20(2)
Rb(21)–$O(12)^{viii}$: 2.95(2)
Rb(21)–$O(17)^{iv}$: 3.36(2)

TABLE 3—*Continued*

Rb(22)–$O(3)^{ii}$: 3.12(2)
Rb(22)–$O(6)^{iv}$: 3.20(2)
Rb(22)–O(7): 3.26(2)
Rb(22)–$O(12)^{viii}$: 3.16(2)
Rb(22)–$O(15)^{iv}$: 3.21(2)
Rb(22)–$O(16)^{vii}$: 3.25(2)
Rb(22)–$O(17)^{vii}$: 3.31(2)

Symmetry codes

i: $1/2+x; 1/2-y; 1/2+z$
ii: $1/2-x; 1/2+y; 1/2-z$
iii: $-1-x; -1-y; -1-z$
iv: $-1/2+x; -3/2-y; -3/2+z$
v: $3/2-x; 1/2+y; 1/2-z$
vi: $-1/2-x; 1/2-y; -1/2+z$
vii: $-1/2+x; y; z$
viii: $1-x; -y; 1-z$

Note: The Mo–O or P–O distances are on the diagonal, above it are the O ··· O distances, and below are the O–Mo–O or O–P–O angles.

c/2 with respect to each other (Fig. 2b) in such a way that the octahedra of one layer are connected with the tetrahedra of the next forming the complex tridimensional framework $[Mo_2WP_3O_{17}]_\infty$. Consequently, each PO_4 tetrahedron shares its four apices with MO_6 octahedra; each isolated *M*(3) octahedron has one free apex (O(12)), but each bioctahedral unit has three free apices (O(7) and O(8)) for *M*(2) and (O(1)) for *M*(1).

The projection of the structure onto the (100) plane (Fig. 3) also shows the existence of large tunnels running along **a** where rubidium cations Rb(2) are located. It is worth pointing out that the "b" and "a" tunnels can communicate through very large windows, but do not intersect each other, in contrast to intersecting tunnel structures like pyrochlores. Note also that the free apices of the MO_6 octahedra are directed toward the axes of the tunnels as well

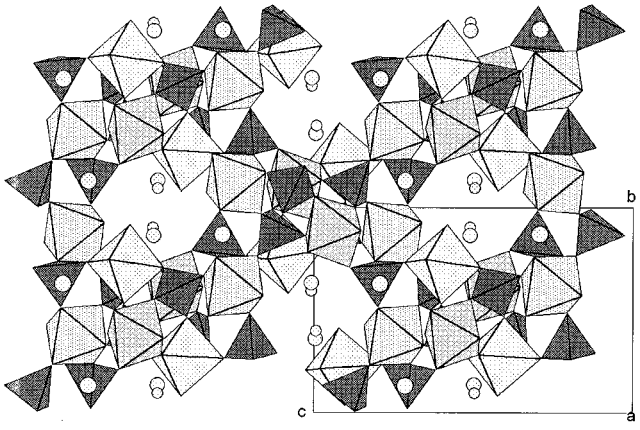

FIG. 3. The projection of the structure of $Rb_2Mo_2WP_3O_{17}$ onto the (100) plane showing large tunnels running along **a**.

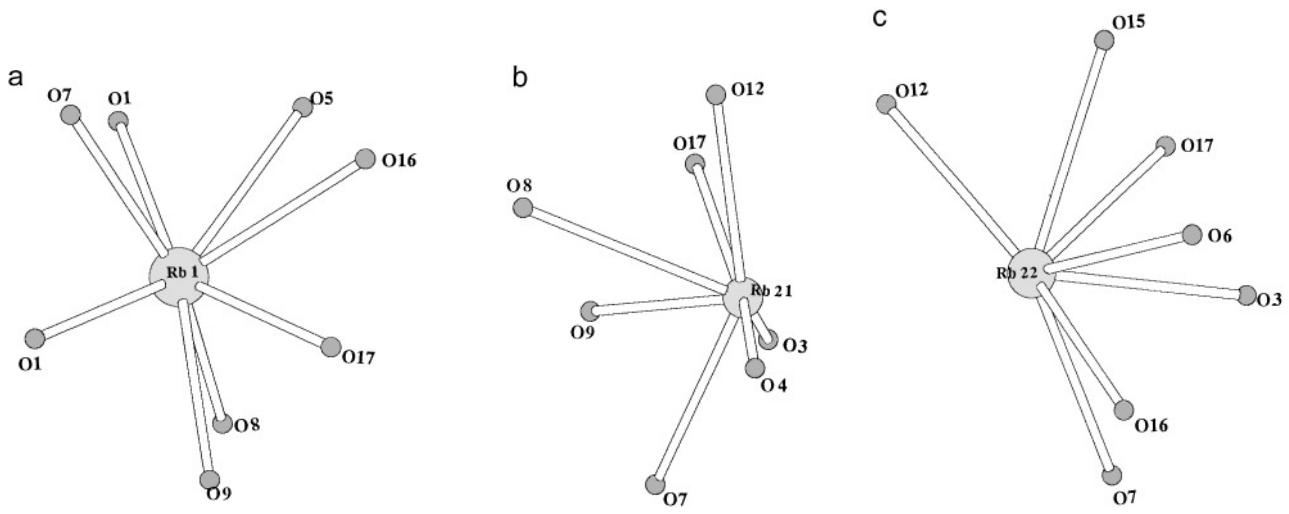

FIG. 4. The surrounding of the rubidium cations.

for the bioctahedral units as for the single MO_6 octahedra (Figs. 1 and 3).

The interatomic distances and bond angles (Table 3) show that the PO_4 tetrahedra exhibit the classical geometry of monophosphate groups, with P–O distances ranging from 1.51 to 1.55 Å. The $M(1)$ and $M(2)$ octahedra that form the bioctahedral units are significantly distorted with three sets of M–O distances: two short M–O bonds of 1.68–1.70 Å and 1.71–1.73 Å for $M(1)$ and $M(2)$, respectively, three intermediate M–O bonds ranging from 1.90 to 2.08 Å, and one longer M–O bond of 2.17 Å for $M(1)$ and 2.25 Å for $M(2)$. This geometry, that is often observed in tungstates and molybdates suggests that the $M(1)$ and $M(2)$ sites are occupied by W(VI) and Mo(VI). In contrast, the $M(3)$ octahedra that are preferentially occupied by molybdenum exhibit a geometry similar to that observed for Mo(V) phosphates. One indeed observes a very short M–O distance of 1.68 Å corresponding to the free apex, whereas the opposite M–O distance is the longest (2.14 Å), the four other equatorial distances being intermediate (1.99–2.04 Å). From this distribution of the M–O distances we can propose a preferential occupancy of the bioctahedral units by the hexavalent species, whereas the isolated $M(3)$ octahedra would be occupied by the pentavalent species according to the formula

$$Rb_2(Mo^{VI}_{0.428}W^{VI}_{0.572})_{M(1)}(Mo^{VI}_{0.672}W^{VI}_{0.328})_{M(2)}\cdot$$

$$(Mo^{V}_{0.883}W^{V}_{0.117})_{M(3)}O_5(PO_4)_3.$$

The Rb–O distances are rather large in agreement with the high thermal factors observed for these cations. The Rb(1) cations that are located in the [010] tunnels are surrounded by eight oxygen atoms forming a distorted archimedian antiprism (Fig. 4a). Note that only three Rb(1)–O distances are smaller than 3 Å, which explains that the thermal factor remains at 2.19 $Å^2$. The coordination of the Rb(2) atoms located near the walls of the [100] tunnels is remarkable. The two sites available Rb(21) and Rb(22) lead to a sevenfold coordination with all the oxygen atoms located on the same side of a plane containing the Rb(2) cation (Figs. 4b and 4c); moreover one observes that all the Rb(2)–O distances are larger than 3 Å. This explains the much higher thermal factors (3.4–3.9 $Å^2$) observed for these cations.

In conclusion, a mixed valent molybdenotungsten monophosphate containing rubidium has been synthesized for the first time. The important characteristic of this new complex structure deals with the existence of large interconnected tunnels where the rubidium cations are located. The large Rb–O distances, as well as the high thermal factors of rubidium, suggest possible mobility of these cations. With respect to this, ion exchange properties and ionic conductivity of this structural type will be studied. Moreover this study opens the route to the systematic research of new phases, with large tunnels by introducing large cations such as rubidium and cesium in the systems A–Mo–W–P–O.

REFERENCES

1. R. C. Haushalter and L. A. Mundi, *Chem. Mater.* **4,** 31 (1992).
2. G. Costentin, A. Leclaire, M-M. Borel, A. Grandin, and B. Raveau, *Rev. Inorg. Chem.* **13,** 77 (1993).
3. M-M. Borel, M. Goreaud, A. Grandin, Ph. Labbé, A. Leclaire, and B. Raveau, *Eur. J. Solid State Inorg. Chem.* **28,** 93 (1991).
4. E. Canadell, Idriss el-Idrisis Rachidi, E. Wang, M. Greenblatt, and M. H. Whango, *Inorg. Chem.* **28,** 2455 (1989).

5. A. Leclaire, M-M. Borel, J. Chardon, and B. Raveau, *J. Solid State Chem.* **120,** 353 (1995).
6. A. Leclaire, M-M. Borel, J. Chardon, and B. Raveau, *J. Solid State Chem.* **124,** 224 (1996).
7. A. Leclaire, M-M. Borel, J. Chardon, and B. Raveau, in press.
8. A. Leclaire, M-M. Borel, J. Chardon, and B. Raveau, *Mater. Res. Bull.* **31,** 1257 (1996).
9. A. Leclaire, M-M. Borel, J. Chardon, and B. Raveau, *J. Solid State Chem.* **127,** 1 (1996).
10. A. Leclaire, M-M. Borel, J. Chardon, and B. Raveau, *Mater. Res. Bull.* **30,** 1075 (1995).